Applied Physics Letters

Spintronics with compensated ferrimagnets

Cite as: Appl. Phys. Lett. **116**, 110501 (2020); https://doi.org/10.1063/1.5144076
Submitted: 03 January 2020 • Accepted: 07 March 2020 • Published Online: 19 March 2020

Joseph Finley and Luqiao Liu

AIP Publishing

Applied Physics Letters PERSPECTIVE scitation.org/journal/apl

Spintronics with compensated ferrimagnets

Cite as: Appl. Phys. Lett. **116**, 110501 (2020); doi: 10.1063/1.5144076
Submitted: 3 January 2020 · Accepted: 7 March 2020 ·
Published Online: 19 March 2020

Joseph Finley and Luqiao Liu[a)]

AFFILIATIONS

Department of Electrical Engineering and Computer Science, Massachusetts Institute of Technology, Cambridge, Massachusetts 02139, USA

[a)]Author to whom correspondence should be addressed: luqiao@mit.edu

ABSTRACT

Magnetic information storage has been achieved by controlling and sensing the magnetic moment orientation of nanoscale ferromagnets. Recently, there has been concentrated effort to utilize materials with antiferromagnetic coupling as a storage medium to realize devices that switch faster, are more secure against external magnetic fields, and have higher storage density. Within this class of materials are ferrimagnets, whose magnetization can be reduced to zero by tuning parameters such as the chemical composition, temperature, and strain. Compared to conventional antiferromagnets, compensated ferrimagnets not only possess the aforementioned speed and density advantages but also allow the use of convenient electrical reading and writing mechanisms due to the existence of inequivalent magnetic sublattices. Recent research has demonstrated fast spin-torque switching, as well as efficient electrical reading with compensated ferrimagnets. Further material and device research using these zero-moment magnets promises a spintronic platform for fast and energy efficient information storage technology.

Modern computer architectures use a memory hierarchy to satisfy trade-offs between speed, latency, energy consumption, retention time, and cost. The emergence of spin-transfer-torque magnetic random access memory (STT-MRAM) provides a possibility to combine high energy-efficiency, large density, long endurance, and non-volatility into a single memory type.[1,2] One direction to further improve the performance of STT-MRAM is to reduce its accessing time, particularly the writing time. The switching process of STT-MRAM occurs when a spin-polarized current is generated in one electrode of a magnetic tunnel junction (MTJ), which then applies a spin-torque that counteracts magnetic damping in the adjacent electrode.[3,4] In this so-called "anti-damping switching" process, the switching speed is governed by the underlying law of angular momentum conservation, particularly in the short pulse switching regime (writing pulse length <10 ns), which states that the switching time is given by the ratio between the total angular momentum of the storage layer and the applied spin current.[5] Therefore, one efficient path for increasing the switching speed is to reduce the total angular momentum in the free magnetic layer, without sacrificing its thermal stability.

Antiferromagnets represent a natural candidate for realizing magnetic materials with low net angular momentum, as they are composed of magnetic sublattices with spins that have antiparallel exchange coupling.[6,7] Beyond the potential increased switching speed, the reduced magnetization also has the added benefit of smaller stray fields, which avoids the undesirable magnetic dipole coupling between neighboring devices, resulting in a higher device density. Materials with antiferromagnetic coupling also typically have a weaker response to magnetic fields, leading to a state that is protected from external magnetic perturbations. Despite these known advantages, one traditional difficulty associated with the usage of antiferromagnets as active components in spintronic devices is the lack of mechanisms for realizing efficient reading and writing. Very recently, experimental progress has been reported in the electrical control and probing of antiferromagnetic states using spin–orbit torque (SOT) and anisotropic magnetoresistance (AMR) [as well as the planar Hall effect (PHE)], in both conductors and insulators,[8–11] providing hope for addressing the long-known obstacles in antiferromagnet spintronics. Alternatively, ferrimagnets serve as another material candidate for reaching the speed and density advantages. Ferrimagnets possess antiferromagnetic sublattices; however, in contrast to antiferromagnets, the two magnetic sublattices do not necessarily have the same magnetic moment or consist of the same atomic species. Instead, the sublattices are inequivalent, lowering the overall symmetry of the material (see Table I). Typically, the magnetization of a ferrimagnet can be varied by changing the ferrimagnet's chemical composition or temperature. In some ferrimagnets, it is possible to reach a state with zero net magnetization, known as the magnetic compensation state. Even though the magnetization can be compensated, the two sublattices are still inequivalent, yielding different densities of states for the two subbands (Table I). This makes it possible to detect magnetic states of a compensated

TABLE I. Comparison between Ferromagnets, antiferromagnets, and ferrimagnets.

	Ferromagnet	Antiferromagnet	Ferrimagnet
Spin structure	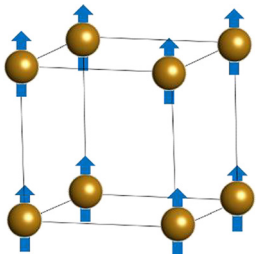	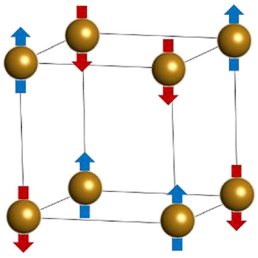	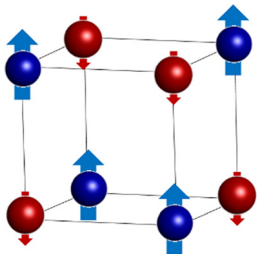
Density of states	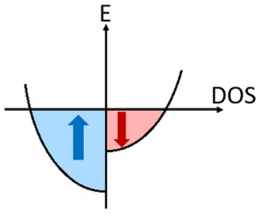	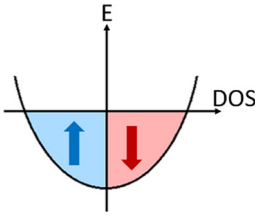	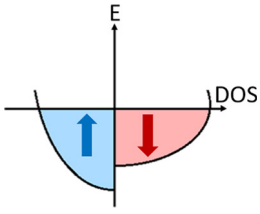
Reading mechanism	Anomalous Hall effect, tunneling magnetoresistance, etc.	(Tunneling) anisotropy magnetoresistance, Planar Hall effect, etc.	Anomalous Hall effect, tunneling magnetoresistance, etc.
Writing mechanism	Spin-transfer torque, spin–orbit torque, E-field control, etc.	Spin–orbit torque, etc.	Spin-transfer torque, spin–orbit torque, etc.

ferrimagnet using similar optical and electrical methods that have been traditionally used for ferromagnets, such as the magneto-optical Kerr effect (MOKE), anomalous Hall effect (AHE), and tunnel magnetoresistance (TMR). In contrast, antiferromagnets have equivalent sublattices and higher symmetry, which results in equal density of states at the Fermi level and zero spin polarization.

One category of well-known ferrimagnets is the rare-earth (RE) transition metal (TM) alloy. RE-TM alloys consist of TM elements (Fe, Co, and Ni) and RE elements (Gd, Tb, etc.) that have magnetic moments originating from electrons on the d and f orbitals, respectively.[12,13] The exchange interaction between d and f electrons can lead to antiferromagnetic coupling for certain combinations of RE-TM alloys.[14] For a given temperature, the net magnetization is determined by the relative concentration of each element, making these materials highly tunable. In these alloys, the electronic density of states at the Fermi level is usually dominated by d electrons from the TM atoms, indicating that the TM solely determines magnetic-related transport properties, providing a way for electrically reading the magnetic state, even at the magnetic compensation state. Meanwhile, the spin–orbit torque from heavy metals (Ta, Pt, etc.)[15,16] or topological insulators,[17–19] which has been used to switch ferromagnets,[20,21] can be used as a mechanism for switching these ferrimagnets as well. Figures 1(a) and 1(b) show the magnetization curve and spin–orbit torque switching curve obtained from a Ta(5)/$Co_{0.79}Tb_{0.21}$ (2)/Ru(3) sample (unit in nanometers; the material composition reflects the atomic ratio).[22] While the sample has a negligible magnetic moment, clear anomalous Hall resistance and current induced switching have been achieved.

In general, the magnetic dynamics of a ferrimagnet with two sublattices is governed by a pair of coupled Landau–Lifshitz–Gilbert (LLG) equations.[23] Under the assumption that the exchange field between the two sublattices is much stronger compared to any other relevant field, the magnetic moment direction of the two sublattices can be approximated as $\hat{\boldsymbol{m}}_{\boldsymbol{A}} = -\hat{\boldsymbol{m}}_{\boldsymbol{B}}$. The dynamics of the net magnetic moment can be obtained by adding the two LLG equations, which leads to[24–26]

$$M_{net}\frac{\mathrm{d}\hat{\boldsymbol{m}}_{\boldsymbol{net}}}{\mathrm{d}t} = -\gamma_{eff}M_{net}\hat{\boldsymbol{m}}_{\boldsymbol{net}} \times \boldsymbol{H}_{\boldsymbol{eff}} + \alpha_{eff}M_{net}\hat{\boldsymbol{m}}_{\boldsymbol{net}} \times \frac{\mathrm{d}\boldsymbol{m}_{\boldsymbol{net}}}{\mathrm{d}t} + \gamma_{eff}J_s\hat{\boldsymbol{m}}_{\boldsymbol{net}} \times (\boldsymbol{\sigma} \times \hat{\boldsymbol{m}}_{\boldsymbol{net}}). \quad (1)$$

Here, M_{net}, $\hat{\boldsymbol{m}}_{\boldsymbol{net}}$, γ_{eff}, α_{eff}, $\boldsymbol{\sigma}$, and $J_{s,\mathrm{tot}}$ are the magnitude of net magnetic moment, direction vector of net magnetic moment, effective gyromagnetic ratio, effective damping coefficient, orientation of injected spin, and total spin current. Specifically, $\boldsymbol{m}_{\boldsymbol{net}} = M_{net}\hat{\boldsymbol{m}}_{\boldsymbol{net}} = \boldsymbol{m}_{\boldsymbol{A}} + \boldsymbol{m}_{\boldsymbol{B}}$ and $\gamma_{eff} = (m_A - m_B)\left(\frac{m_A}{\gamma_A} - \frac{m_B}{\gamma_B}\right)^{-1}$, where $\gamma_{A(B)}$ is the gyromagnetic ratio of the two sublattices. It is known that the gyromagnetic ratio of TM and RE metals could be slightly different due to the unequal contributions from orbital magnetism in these two types of atoms. From this equation, it can be seen that the spin torque term $\boldsymbol{\tau}_{\boldsymbol{ST}} = J_s\hat{\boldsymbol{m}}_{\boldsymbol{net}} \times (\boldsymbol{\sigma} \times \hat{\boldsymbol{m}}_{\boldsymbol{net}})$ is independent of the net magnetic moment in the ferrimagnetic material, consistent with the angular momentum conservation picture. Experimentally to quantify the spin–orbit torque, it is usually convenient to compare the effect generated from a spin torque with that from an applied magnetic field, using the DC domain wall magnetometry method[27] or high harmonic measurement[28,29] (see Table II). From Eq. (1), by comparing the terms for the spin torque and the field induced torque, one can see that the effective field from $\boldsymbol{\tau}_{\boldsymbol{ST}}$ has the magnitude of $\frac{J_s}{M_{net}}$, which diverges at the magnetization compensation point. This large increase in the (dampling-like) spin–orbit torque effective field has been verified in several experiments,[22,30–35] which is summarized in Table II. One emphasis that needs to be made is that in real magnetic memory devices, the

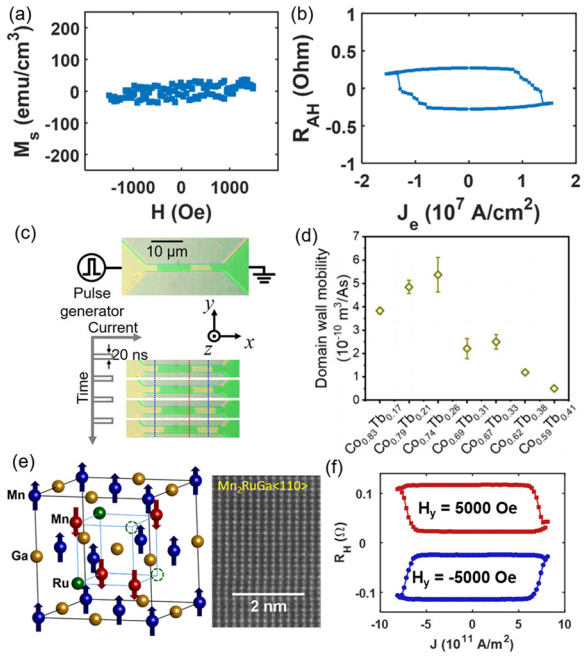

FIG. 1. (a) Magnetization curve and (b) spin–orbit torque switching curve for a Ta(5)/$Co_{0.79}Tb_{0.21}$(2)/Ru(3) sample (unit in nanometers). Reproduced with permission from J. Finley and L. Liu, Phys. Rev. Appl. **6**, 054001 (2016). Copyright 2016 American Physical Society. Although the sample has negligible magnetization, clear anomalous Hall resistance can be measured and current-induced switching has been achieved. (c) Spin–orbit torque induced domain wall motion measurement of CoTb(3)/Pt(5) (unit in nanometers) using MOKE. (d) Highest domain wall mobility occurs near the angular momentum compensation point and is much larger than a typical ferromagnetic material. Reproduced with permission from Siddiqui *et al.*, Phys. Rev. Lett. **121**, 057701 (2018). Copyright 2018 American Physical Society. (e) Crystal structure and high resolution scanning transmission electron microscope (STEM) image of the ferrimagnetic Heusler alloy Mn_2GaRu_x. (f) Spin–orbit torque switching of a nearly compensated $Mn_2GaRu_{0.68}$(23)/Pt(5) film (unit in nanometers). Reproduced with permission from Finley *et al.*, Adv. Mater. **31**, 1805361 (2019). Copyright 2019 John Wiley and Sons.

requirement of a high energy barrier against thermal fluctuation $E = M_{net}H_c$ determines that the coercive field of a ferrimagnet H_c also needs to be very high when the net magnetization is reduced to zero. Under this restraint, H_c scales as $1/M_{net}$, which compensates the decrease in the threshold current brought by the divergences of the spin torque effective field discussed above.

While the divergence of the effective field from spin torque at the magnetization compensation point does not directly lead to a more efficient magnetic memory, there could be switching speed advantages associated with the usage of ferrimagnets. From Eq. (1), it can be seen that the changing rate of the magnetic moment direction under spin torque has the following form: $\frac{d\hat{\boldsymbol{m}}_{net}}{dt} \sim \gamma_{eff}\frac{J_{s,tot}}{M_{net}}\hat{\boldsymbol{m}}_{net} \times (\boldsymbol{\sigma} \times \hat{\boldsymbol{m}}_{net})$, which becomes large when $\gamma_{eff}{M_{net}}^{-1} = (\frac{m_A}{\gamma_A} - \frac{m_B}{\gamma_B})^{-1}$ diverges at the angular momentum compensation point. Here, the net angular momentum $S_{net} = S_A - S_B = \frac{m_A}{\gamma_A} - \frac{m_B}{\gamma_B}$. This trend has been recently observed in current-induced domain wall motion experiments, where it was shown that domain wall velocity is maximized at the angular momentum compensation point[36–38] [see Figs. 1(c) and 1(d)]. Particularly, with CoGd alloys, Caretta *et al.* and Cai *et al.* demonstrated domain wall velocities above 1 km/s, which is more than an order of magnitude larger than that in traditional ferromagnets.[37,38] The peak domain wall velocity observed at the angular momentum compensation point can be explained by considering the spin torque effective field generated in the domain wall region.[39] The absence of the internal magnetic texture change at a high applied current, known as Walker breakdown, is believed to be the direct cause of a larger domain wall velocity in ferrimagnets with nearly zero angular momentum.

Being a well-studied material system, RE-TM alloys allow people to carry out a series of proof-of-concept experiments, which show many interesting physics close to the angular momentum or magnetic momentum compensation point. However, the strong temperature dependence of magnetic moment, potential damping enhancement, and active chemical properties brought by RE elements[40–43] pose great challenges for real applications. Particularly, because of the low electronegativity, REs, in their metallic state, are very easy to oxidize by

TABLE II. Comparison of spin–orbit torque measurements on compensated ferrimagnets.

Material (thickness in nm)	Measurement type	Effective field from damping-like torque	Effective field from field-like torque (10^{-7} Oe $A^{-1}cm^2$)	Effective spin Hall angle
CoTb(2)/Ta(5)[22]	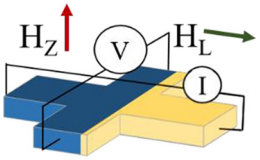	$1/M_s$	…	0.03
CoTb(3.5)/W(3)[34]		$1/M_s$	…	0.26
	Hall Shift			
CoTb(6.5)/Ta(8)[30]	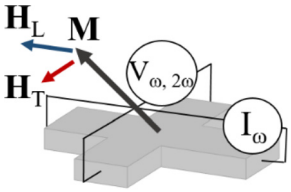	$1/M_s$	~15	0.10
Pt(5)/CoFeGd(30)/Ta(5)[31]		$1/M_s$	~20	0.187
CoFeGd(10)/Pt(5)[32]		$1/M_s$	…	0.014
CoGd(6)/Pt(10)[33]		$1/M_s^2$	~500	0.52
CoFeGd(15)/Bi_2Se_3(6), $(BiSb)_2Te_3$(6)[35]		$1/M_s$	…	0.13, 3.01
Mn_2GaRu_x(23)/Pt(5)[62]		…	~7	0.025
	Harmonic Hall			

adjacent oxide films such as MgO, which usually leads to very poor tunneling magnetoresistance (TMR) in magnetic tunnel junctions (MTJs) containing these ferrimagnets.[44] Beyond RE-TM alloys, some members in the family of Heusler alloys also possess tunable ferrimagnetism. Heusler alloys are a large group of intermetallic compounds that consist of up to four different elements and can form several different crystal structures (Table III). With many possible elemental permutations, it is possible to engineer properties such as magnetic order, half metallicity, multiferroicity, topological order, and net magnetic moment in these materials.[45] In fact, compensated Heusler alloys have recently been studied as a ferrimagnetic exchange bias layer in magnetic devices due to the large coercive field close to the zero magnetization point.[46,47] In addition to magnetization compensation, half metallicity is another appealing property that can benefit spintronic applications. Half metallicity represents the state where one spin subband is conducting, while the other is insulating.[48] In principle, half-metallicity can co-exist with zero magnetization in a ferrimagnet. The expected 100% spin polarization in certain Heusler alloys can lead to MTJs with extremely large TMR.[49] In addition to high spin polarization, half metallicity can also reduce magnetic damping by avoiding electron spin flip scattering, which is particularly useful for various spintronic applications, as this can reduce switching thresholds, increase domain wall velocities, and lead to a narrower linewidth in magnetic oscillation.[50,51] Combining compensated ferrimagnetism, improved thermal stability, ultra-low damping, and 100% spin polarization into a single material is therefore an intriguing prospect of the study on Heusler alloys. First principles calculations show that ferrimagnets with low magnetic moment can be realized in Mn-rich Heusler alloys, e.g., Mn_3Ga, Mn_2PtGa, Mn_2RuGa, etc. It was demonstrated that the Slater–Pauling rule,[52,53] the empirical formula which predicts the magnetic moment per atom in 3d transition metals, also gives a useful guideline on the design of magnetization in Heusler alloys.[45,54–57] Zero net magnetic moment can be achieved by tuning the number of valence electrons via adjusting the chemical composition and concentration of different elements. H. Kurt *et al.* proposed and verified this concept by carefully controlling the phase and chemical composition of an exemplar Heusler alloy system $Mn_2Ru_{1-x}Ga$.[58] By varying the relative concentration between Mn and Ru elements, they showed that the magnetic moment of $Mn_2Ru_{1-x}Ga$ can be compensated at room temperature. Preliminary experimental results also suggest that there could be half-metallicity around this compensation point. Unlike many other low moment Heusler alloys that crystalize in tetragonal structures,[46,49,59–61] $Mn_2Ru_{1-x}Ga$ epitaxially grown on a MgO substrate exhibits a cubic crystal structure [as seen in Fig. 1(e)], resulting in relatively weaker crystalline anisotropy. This moderate perpendicular anisotropy makes $Mn_2Ru_{1-x}Ga$ a good candidate as a free layer in spintronic devices. In a recent experiment, it was shown that by utilizing the spin Hall effect from an adjacent Pt layer, spin–orbit torque induced switching can be realized in $Mn_2Ru_{1-x}Ga$ very close to the magnetization compensation point [Fig. 1(f)].[62] Similar to RE-TM alloys, it is reasonable to believe that fast switching dynamics will occur in these low moment Heusler ferrimagnets. Recent experiments on the fast domain wall motion from ferrimagnetic Heusler films provide initial evidence along this direction.[63]

The above discussion only reflects a small subset of research that is being pursued in the field of compensated ferrimagnetic materials. Beyond the study of RE-TM alloys and Heusler alloys, there is also extensive interest in ferrimagnetic garnets (Table III), which have been shown to have magnetization compensation close to room temperature,[64,65] be switchable with spin–orbit torque,[66] and exhibit ultra-fast domain wall motion.[67] The insulating nature of these garnets can potentially improve the energy efficiency by eliminating part of Joule-heating related dissipation in spintronic devices. In addition to the ferrimagnetic switching dynamics studied in the single domain and domain wall motion regime, it has also been shown that interesting physics can occur with topologically protected magnetic quasi-particles—skyrmions. Experiments have shown that the Dzyaloshinskii–Moriya interaction (DMI) acts on the two sublattices of ferrimagnets constructively instead of canceling each other close to the compensation point. Therefore, chiral domain wall structures can be realized in a zero moment magnet due to the sizable DMI effective field.[36] It has been shown in both theory and experiment that compared to ferromagnets, the reduced stray fields in compensated ferrimagnets allow much smaller skyrmions to be formed.[37,68] Furthermore, current-induced skyrmion motion can exhibit higher speeds in compensated ferrimagnets than in regular ferromagnets due to the reduction of current-induced transverse velocity (i.e., the skyrmion Hall effect).[69,70] Finally, compensated ferrimagnets have also been an essential component for achieving all optical switching.[71] Ultrafast picosecond laser induced magnetic switching has been demonstrated in ferrimagnets with very low magnetic moments.[71–74]

While the uncompensated electron density of states at the Fermi surface of ferrimagnets provides advantageous mechanisms for

TABLE III. Comparison between different ferrimagnetic materials.

	Transition metal rare-earth alloy	Heusler alloy	Rare-earth iron garnet
Crystal structure	Amorphous	Heusler, half Heusler, inverse Heusler	Garnet
Examples	CoGd, CoTb, CoFeGd, etc.	Mn_3Ga, Mn_3Ge, Mn_2GaRu_x, Mn_2GaPt_x, etc.	$Gd_3Fe_5O_{12}$, $Tm_3Fe_5O_{12}$, $Tb_3Fe_5O_{12}$, $Eu_3Fe_5O_{12}$, etc.
Reading mechanisms	Anomalous Hall effect tunneling magnetoresistance: (low TMR ratio)	Anomalous Hall effect tunneling magnetoresistance: (the high TMR ratio remains to be demonstrated)	Spin Hall magnetoresistance
Writing mechanisms	STT and SOT	STT and SOT	SOT
Compensation mechanisms	Temperature and chemical composition	Temperature, chemical composition, and strain	Temperature and strain

magnetic reading and writing over antiferromagnets, the dependence of the compensation condition on the exact position of the Fermi level also brings about disadvantages for applications. Particularly, the magnetic properties of ferrimagnets, including net moment, magnetic anisotropy, etc., usually have a strong temperature dependence, in contrast to antiferromagnets, where the moment is always rigorously zero regardless of the temperature (see Table I). As a matter of fact, many of the experiments discussed in this perspective article utilize this temperature dependence to reach magnetic or angular momentum compensation. One can easily imagine that it will be technically difficult to maintain a fixed temperature for real device applications. Therefore, compensated ferrimagnetic materials with more robust temperature stability will be highly preferred in future development. Moreover, TMR is one of the best known methods for fast, reliable magnetic reading. While using compensated ferrimagnets can, in principle, lead to large TMR, in existing reports of MTJs made from various compensated ferrimagnets, they still suffer from low ON/OFF ratios, probably related to certain chemical or structural imperfections.[49,75] Demonstrating a TMR ratio that is comparable to or even larger than existing CoFeB based MTJs will be another important question to address in future studies on compensated ferrimagnets.

So far, current induced magnetic switching has been realized in compensated ferrimagnets, where it was found that the spin-torque effective field is inversely proportional to magnetization. Fast domain wall motion was realized near the angular momentum compensation point, and compensated Heusler alloys with low damping and high spin polarization have been electrically switched. By building on these results with continuous research into materials and the underlying physics, compensated ferrimagnets promise an exciting platform for a fast and energy efficient information storage technology.

REFERENCES

[1]A. D. Kent and D. C. Worledge, Nat. Nanotechnol. **10**, 187 (2015).
[2]H.-S. P. Wong and S. Salahuddin, Nat. Nanotechnol. **10**, 191 (2015).
[3]J. C. Slonczewski, J. Magn. Magn. Mater. **159**, L1 (1996).
[4]L. Berger, Phys. Rev. B **54**, 9353 (1996).
[5]J. Z. Sun, Phys. Rev. B **62**, 570 (2000).
[6]T. Jungwirth, X. Marti, P. Wadley, and J. Wunderlich, Nat. Nanotechnol. **11**, 231 (2016).
[7]V. Baltz, A. Manchon, M. Tsoi, T. Moriyama, T. Ono, and Y. Tserkovnyak, Rev. Mod. Phys. **90**, 015005 (2018).
[8]P. Wadley, B. Howells, J. Železný, C. Andrews, V. Hills, R. P. Campion, V. Novák, K. Olejník, F. Maccherozzi, S. S. Dhesi, S. Y. Martin, T. Wagner, J. Wunderlich, F. Freimuth, Y. Mokrousov, J. Kuneš, J. S. Chauhan, M. J. Grzybowski, A. W. Rushforth, K. W. Edmonds, B. L. Gallagher, and T. Jungwirth, Science **351**, 587–590 (2016).
[9]S. Y. Bodnar, L. Šmejkal, I. Turek, T. Jungwirth, O. Gomonay, J. Sinova, A. A. Sapozhnik, H.-J. Elmers, M. Kläui, and M. Jourdan, Nat. Commun. **9**, 348 (2018).
[10]T. Moriyama, K. Oda, T. Ohkochi, M. Kimata, and T. Ono, Sci. Rep. **8**, 14167 (2018).
[11]X. Z. Chen, R. Zarzuela, J. Zhang, C. Song, X. F. Zhou, G. Y. Shi, F. Li, H. A. Zhou, W. J. Jiang, F. Pan, and Y. Tserkovnyak, Phys. Rev. Lett. **120**, 207204 (2018).
[12]R. C. O'Handley, *Modern Magnetic Materials: Principles and Applications* (Wiley, New York, NY, 2000).
[13]P. J. Grundy, "High density magneto-optical recording materials," in *Materials Science and Technology* (Wiley, 2006).
[14]I. A. Campbell, J. Phys. F **2**, L47 (1972).
[15]M. I. Dyakonov and V. I. Perel, Phys. Lett. A **35**, 459 (1971).
[16]J. E. Hirsch, Phys. Rev. Lett. **83**, 1834 (1999).
[17]Y. Fan, P. Upadhyaya, X. Kou, M. Lang, S. Takei, Z. Wang, J. Tang, L. He, L.-T. Chang, M. Montazeri, G. Yu, W. Jiang, T. Nie, R. N. Schwartz, Y. Tserkovnyak, and K. L. Wang, Nat. Mater. **13**, 699 (2014).
[18]A. R. Mellnik, J. S. Lee, A. Richardella, J. L. Grab, P. J. Mintun, M. H. Fischer, A. Vaezi, A. Manchon, E.-A. Kim, N. Samarth, and D. C. Ralph, Nature **511**, 449 (2014).
[19]J. Han, A. Richardella, S. A. Siddiqui, J. Finley, N. Samarth, and L. Liu, Phys. Rev. Lett. **119**, 077702 (2017).
[20]I. M. Miron, K. Garello, G. Gaudin, P.-J. Zermatten, M. V. Costache, S. Auffret, S. Bandiera, B. Rodmacq, A. Schuhl, and P. Gambardella, Nature **476**, 189 (2011).
[21]L. Liu, C.-F. Pai, Y. Li, H. W. Tseng, D. C. Ralph, and R. A. Buhrman, Science **336**, 555 (2012).
[22]J. Finley and L. Liu, Phys. Rev. Appl. **6**, 054001 (2016).
[23]R. K. Wangsness, Phys. Rev. **91**, 1085 (1953).
[24]M. Binder, A. Weber, O. Mosendz, G. Woltersdorf, M. Izquierdo, I. Neudecker, J. R. Dahn, T. D. Hatchard, J.-U. Thiele, C. H. Back, and M. R. Scheinfein, Phys. Rev. B **74**, 134404 (2006).
[25]C. D. Stanciu, A. V. Kimel, F. Hansteen, A. Tsukamoto, A. Itoh, A. Kirilyuk, and T. Rasing, Phys. Rev. B **73**, 220402 (2006).
[26]X. Jiang, L. Gao, J. Z. Sun, and S. S. P. Parkin, Phys. Rev. Lett. **97**, 217202 (2006).
[27]C.-F. Pai, M. Mann, A. J. Tan, and G. S. D. Beach, Phys. Rev. B **93**, 144409 (2016).
[28]U. H. Pi, K. Won Kim, J. Y. Bae, S. C. Lee, Y. J. Cho, K. S. Kim, and S. Seo, Appl. Phys. Lett. **97**, 162507 (2010).
[29]J. Kim, J. Sinha, M. Hayashi, M. Yamanouchi, S. Fukami, T. Suzuki, S. Mitani, and H. Ohno, Nat. Mater. **12**, 240 (2013).
[30]K. Ueda, M. Mann, P. W. P. de Brouwer, D. Bono, and G. S. D. Beach, Phys. Rev. B **96**, 064410 (2017).
[31]N. Roschewsky, C.-H. Lambert, and S. Salahuddin, Phys. Rev. B **96**, 064406 (2017).
[32]W. Seung Ham, S. Kim, D.-H. Kim, K.-J. Kim, T. Okuno, H. Yoshikawa, A. Tsukamoto, T. Moriyama, and T. Ono, Appl. Phys. Lett. **110**, 242405 (2017).
[33]R. Mishra, J. Yu, X. Qiu, M. Motapothula, T. Venkatesan, and H. Yang, Phys. Rev. Lett. **118**, 167201 (2017).
[34]S.-G. Je, J.-C. Rojas-Sánchez, T. H. Pham, P. Vallobra, G. Malinowski, D. Lacour, T. Fache, M.-C. Cyrille, D.-Y. Kim, S.-B. Choe, M. Belmeguenai, M. Hehn, S. Mangin, G. Gaudin, and O. Boulle, Appl. Phys. Lett. **112**, 062401 (2018).
[35]H. Wu, Y. Xu, P. Deng, Q. Pan, S. A. Razavi, K. Wong, L. Huang, B. Dai, Q. Shao, G. Yu, X. Han, J.-C. Rojas-Sánchez, S. Mangin, and K. L. Wang, Adv. Mater. **31**, 1901681 (2019).
[36]S. A. Siddiqui, J. Han, J. T. Finley, C. A. Ross, and L. Liu, Phys. Rev. Lett. **121**, 057701 (2018).
[37]L. Caretta, M. Mann, F. Büttner, K. Ueda, B. Pfau, C. M. Günther, P. Hessing, A. Churikova, C. Klose, M. Schneider, D. Engel, C. Marcus, D. Bono, K. Bagschik, S. Eisebitt, and G. S. D. Beach, Nat. Nanotechnol. **13**, 1154 (2018).
[38]K. Cai, Z. Zhu, J. M. Lee, R. Mishra, L. Ren, S. D. Pollard, P. He, G. Liang, K. L. Teo, and H. Yang, Nat. Electron. **3**, 37 (2020).
[39]A. Thiaville, S. Rohart, É. Jué, V. Cros, and A. Fert, Europhys. Lett. **100**, 57002 (2012).
[40]C. Kaiser, A. F. Panchula, and S. S. P. Parkin, Phys. Rev. Lett. **95**, 047202 (2005).
[41]R. Meservey, D. Paraskevopoulos, and P. M. Tedrow, Phys. Rev. B **22**, 1331 (1980).
[42]P. Hansen, C. Clausen, G. Much, M. Rosenkranz, and K. Witter, J. Appl. Phys. **66**, 756 (1989).
[43]G. Woltersdorf, M. Kiessling, G. Meyer, J.-U. Thiele, and C. H. Back, Phys. Rev. Lett. **102**, 257602 (2009).
[44]M. Nakayama, T. Kai, N. Shimomura, M. Amano, E. Kitagawa, T. Nagase, M. Yoshikawa, T. Kishi, S. Ikegawa, and H. Yoda, J. Appl. Phys. **103**, 07A710 (2008).
[45]T. Graf, C. Felser, and S. S. P. Parkin, Prog. Solid State Chem. **39**, 1 (2011).
[46]A. K. Nayak, M. Nicklas, S. Chadov, P. Khuntia, C. Shekhar, A. Kalache, M. Baenitz, Y. Skourski, V. K. Guduru, A. Puri, U. Zeitler, J. M. D. Coey, and C. Felser, Nat. Mater. **14**, 679 (2015).

[47]R. Sahoo, L. Wollmann, S. Selle, T. Höche, B. Ernst, A. Kalache, C. Shekhar, N. Kumar, S. Chadov, C. Felser, S. S. P. Parkin, and A. K. Nayak, Adv. Mater. **28**, 8499 (2016).
[48]R. A. de Groot, F. M. Mueller, P. G. van Engen, and K. H. J. Buschow, Phys. Rev. Lett. **50**, 2024 (1983).
[49]J. Jeong, Y. Ferrante, S. V. Faleev, M. G. Samant, C. Felser, and S. S. P. Parkin, Nat. Commun. **7**, 10276 (2016).
[50]S. Mizukami, A. Sugihara, S. Iihama, Y. Sasaki, K. Z. Suzuki, and T. Miyazaki, Appl. Phys. Lett. **108**, 012404 (2016).
[51]G. Bonfiglio, K. Rode, K. Siewerska, J. Besbas, G. Y. P. Atcheson, P. Stamenov, J. M. D. Coey, A. V. Kimel, T. Rasing, and A. Kirilyuk, Phys. Rev. B **100**, 104438 (2019).
[52]J. C. Slater, Phys. Rev. **49**, 931 (1936).
[53]L. Pauling, Phys. Rev. **54**, 899 (1938).
[54]J. Kübler, Physica B+C **127**, 257 (1984).
[55]I. Galanakis, P. H. Dederichs, and N. Papanikolaou, Phys. Rev. B **66**, 174429 (2002).
[56]S. Skaftouros, K. Özdoğan, E. Şaşıoğlu, and I. Galanakis, Phys. Rev. B **87**, 024420 (2013).
[57]L. Wollmann, S. Chadov, J. Kübler, and C. Felser, Phys. Rev. B **90**, 214420 (2014).
[58]H. Kurt, K. Rode, P. Stamenov, M. Venkatesan, Y.-C. Lau, E. Fonda, and J. M. D. Coey, Phys. Rev. Lett. **112**, 027201 (2014).
[59]B. Balke, G. H. Fecher, J. Winterlik, and C. Felser, Appl. Phys. Lett. **90**, 152504 (2007).
[60]H. Kurt, K. Rode, M. Venkatesan, P. Stamenov, and J. M. D. Coey, Phys. Rev. B **83**, 020405 (2011).
[61]H. Kurt, N. Baadji, K. Rode, M. Venkatesan, P. Stamenov, S. Sanvito, and J. M. D. Coey, Appl. Phys. Lett. **101**, 132410 (2012).
[62]J. Finley, C.-H. Lee, P. Y. Huang, and L. Liu, Adv. Mater. **31**, 1805361 (2019).
[63]P. C. Filippou, J. Jeong, Y. Ferrante, S.-H. Yang, T. Topuria, M. G. Samant, and S. S. P. Parkin, Nat. Commun. **9**, 4653 (2018).
[64]S. Geprägs, A. Kehlberger, F. D. Coletta, Z. Qiu, E.-J. Guo, T. Schulz, C. Mix, S. Meyer, A. Kamra, M. Althammer, H. Huebl, G. Jakob, Y. Ohnuma, H. Adachi, J. Barker, S. Maekawa, G. E. W. Bauer, E. Saitoh, R. Gross, S. T. B. Goennenwein, and M. Kläui, Nat. Commun. **7**, 10452 (2016).
[65]E. R. Rosenberg, L. Beran, C. O. Avci, C. Zeledon, B. Song, C. Gonzalez-Fuentes, J. Mendil, P. Gambardella, M. Veis, C. Garcia, G. S. D. Beach, and C. A. Ross, Phys. Rev. Mater. **2**, 094405 (2018).
[66]C. O. Avci, A. Quindeau, C.-F. Pai, M. Mann, L. Caretta, A. S. Tang, M. C. Onbasli, C. A. Ross, and G. S. D. Beach, Nat. Mater. **16**, 309 (2017).
[67]C. O. Avci, E. Rosenberg, L. Caretta, F. Büttner, M. Mann, C. Marcus, D. Bono, C. A. Ross, and G. S. D. Beach, Nat. Nanotechnol. **14**, 561 (2019).
[68]F. Büttner, I. Lemesh, and G. S. D. Beach, Sci. Rep. **8**, 4464 (2018).
[69]S. Woo, K. M. Song, X. Zhang, Y. Zhou, M. Ezawa, X. Liu, S. Finizio, J. Raabe, N. J. Lee, S.-I. Kim, S.-Y. Park, Y. Kim, J.-Y. Kim, D. Lee, O. Lee, J. W. Choi, B.-C. Min, H. C. Koo, and J. Chang, Nat. Commun. **9**, 959 (2018).
[70]Y. Hirata, D.-H. Kim, S. K. Kim, D.-K. Lee, S.-H. Oh, D.-Y. Kim, T. Nishimura, T. Okuno, Y. Futakawa, H. Yoshikawa, A. Tsukamoto, Y. Tserkovnyak, Y. Shiota, T. Moriyama, S.-B. Choe, K.-J. Lee, and T. Ono, Nat. Nanotechnol. **14**, 232 (2019).
[71]C. D. Stanciu, F. Hansteen, A. V. Kimel, A. Kirilyuk, A. Tsukamoto, A. Itoh, and T. Rasing, Phys. Rev. Lett. **99**, 047601 (2007).
[72]I. Radu, K. Vahaplar, C. Stamm, T. Kachel, N. Pontius, H. A. Dürr, T. A. Ostler, J. Barker, R. F. L. Evans, R. W. Chantrell, A. Tsukamoto, A. Itoh, A. Kirilyuk, T. Rasing, and A. V. Kimel, Nature **472**, 205 (2011).
[73]S. Mangin, M. Gottwald, C.-H. Lambert, D. Steil, V. Uhlíř, L. Pang, M. Hehn, S. Alebrand, M. Cinchetti, G. Malinowski, Y. Fainman, M. Aeschlimann, and E. E. Fullerton, Nat. Mater. **13**, 286 (2014).
[74]Y. Yang, R. B. Wilson, J. Gorchon, C.-H. Lambert, S. Salahuddin, and J. Bokor, Sci. Adv. **3**, e1603117 (2017).
[75]A. Titova, C. Fowley, E. Clifford, Y.-C. Lau, K. Borisov, D. Betto, G. Atcheson, R. Hübner, C. Xu, P. Stamenov, M. Coey, K. Rode, J. Lindner, J. Fassbender, and A. M. Deac, Sci. Rep. **9**, 4020 (2019).